ELSEVIER

Journal of Chromatography A, 666 (1994) 271–283

JOURNAL OF CHROMATOGRAPHY A

Capillary zone electrophoresis of synthetic opioid and tachykinin peptides

Huey G. Lee[a], Dominic M. Desiderio*[,a,b,c]

[a] *Charles B. Stout Neuroscience Mass Spectrometry Laboratory, University of Tennessee at Memphis, Memphis, TN 38163, USA*

[b] *Department of Neurology, College of Medicine, University of Tennessee at Memphis, 956 Court Avenue, Room A218, Memphis, TN 38163, USA*

[c] *Department of Biochemistry, University of Tennessee at Memphis, Memphis, TN 38163, USA*

(First received September 13th, 1993; revised manuscript received November 11th, 1993)

Abstract

Capillary zone electrophoresis was performed on fourteen synthetic opioid peptides and one tachykinin peptide (substance P = SP) at pH values of 2.5, 5.5 and 8.5 to rationalize the electrophoretic behavior of these neuropeptides. A plot of the theoretical $q/M_r^{2/3}$ values (where q = peptide charge) calculated across the pH range of 1 to 10 for these peptides was used to understand and to predict their separation. The experimentally determined electrophoretic mobilities (μ) were correlated to the estimate of the relative μ predicted by $q/M_r^{2/3}$ and by $[\ln (q+1)]/n^{0.43}$ (where n = number of constituent amino acids), where q values were calculated using amino acid pK_a values for an isolated amino acid and for an amino acid in a peptide. In general, relatively high correlations were obtained with either mathematical expression and with both sets of amino acid pK_a values for data at a single pH value. However, the combination of the former expression and the adjusted pK_a values gave the best prediction of electrophoretic behavior when data for the three pH values were correlated across these different separation conditions.

1. Introduction

Throughout the historical development of capillary zone electrophoresis (CZE), Jorgenson and Lukacs [1,2] were largely responsible for popularizing the technique in the early 1980s by demonstrating its high resolution capability using very narrow open-tubular glass capillaries (< 100 μm I.D.). Those narrow-I.D. capillaries have a high surface area-to-volume ratio that efficiently dissipate the heat (Joule heating) generated by the high voltage and by the buffer resistance. In addition to the important experimental parameter of high electrophoretic resolution that is achievable by CZE, other advantages include detection sensitivity, selectivity, rapid analyses, on-line detection, interfacing to mass spectrometry (MS), long column life, low sample/reagent consumption and automation.

In CZE, an analyte migrates in a capillary by its electrostatic attraction to an anode or cathode in the electric field gradient generated by high

* Corresponding author. Address for correspondence: Department of Neurology, College of Medicine, University of Tennessee at Memphis, 956 Court Avenue, Room A218, Memphis, TN 38163, USA

0021-9673/94/$07.00
SSDI 0021-9673(94)00044-A

voltage. Besides the electrostatic force, the analyte is also transported through the capillary by electroosmotic flow due to the ζ potential that exists between the analytes/electrolytes and the ionized silanols ($pK_a \approx 3.0$) on the inner wall of a glass or fused-silica capillary. The apparent electrophoretic mobility (μ_{app}) of an analyte is therefore equal to its inherent electrophoretic mobility (μ) plus the electroosmotic mobility (μ_{eo}), or,

$$\mu_{app} = \mu + \mu_{eo} \quad (1)$$

From an analyte's perspective, μ is predominantly a direct function of the analyte charge that is attracted by an electrostatic force and an inverse function of its mass, which retards electrophoretic migration due to frictional drag of the molecule against the medium and the silanols on the inner wall of the capillary. Understanding these two inherent physiochemical properties (charge and mass) of the analyte would aid in predicting and optimizing CZE separation. In fact, with various degrees of effort and different objectives, several research groups [3–13] have attempted to investigate this charge-to-mass relationship *vs.* peptide mobility in CZE.

Peptide charge (q) can be readily calculated from known amino acid pK_a values using the Henderson–Hasselbach equation (see ref. 14). In practice, the calculation of a charge on a peptide in a CZE capillary may not be possible, because not only do the pK_a values [9] of isolated amino acids differ from those pK_a values of amino acids in a peptide, but the microenvironment (solvent, dipoles, silanols, buffer) surrounding the peptide and other factors such as peptide hydrophobicity may also play a role in affecting a pK_a value through a change in the dielectric constant of the medium. Furthermore, temperature, viscosity, buffer composition and ionic strength can also affect the degree of ionization of the charged groups. Fortunately, many of these variables and their effects on peptide charge can be maintained nearly constant within an experiment, and thus, the charges calculated for a series of peptides become proportional to each other.

In this study, we investigated the CZE behavior of selected peptides as a function of the charge on the peptides calculated from isolated amino acid pK_a values and from adjusted amino acid pK_a values, using tabulated data from Rickard *et al.* [9]. The adjusted pK_a values were used to compensate for the amount of charge density of the amino acid at each terminus of a peptide because that density is diminished electrostatically by the presence of the first and last peptide bonds.

Because peptides have a limited secondary structure, parameters relative to their size/shape can often be simplified. Such simplifications allow the use of mathematical equations to correlate a peptide mass to peptide μ. Despite the existence of numerous peptide size/shape models, which are summarized by Rickard *et al.* [9], the Offord relationship [15] is the one that has been most studied and confirmed by many researchers [3–6,8–13]. Offord proposed that the retarding shear force that an analyte encounters in a conducting medium for paper electrophoresis is proportional to the analyte's surface area, assuming that the molecule is spherical and smooth. The molecular mass (M_r) of a peptide is used to estimate its size, and the 2/3 power accounts for the mathematical proportionality between area and volume. Thus, μ is correlated to this M_r model by the expression $q/M_r^{2/3}$. On the contrary, Grossman *et al.* [7] treated each peptide as a rod-shaped homopolymer whose size is determined by the number (n) of constituent amino acids, and they obtained high correlation ($r = 0.989$) between a peptide's μ and its charge-to-mass parameter $[\ln(q+1)]/n^{0.43}$ for a series of synthetic peptides. Both theoretical approaches, with an emphasis on the former for the treatment of peptide size/shape, were used in this study.

Potential applications of CZE in biomedical research have been the subject of several recent reviews [16–18]. For many years, this laboratory has been involved in analyzing neuropeptides, and especially opioid and tachykinin neuropeptides, from biological sources including human tissues and fluids by using multi-dimensional reversed-phase high-performance liquid chroma-

tography (RP-HPLC) for sample preparation [19] and using radioimmunoassay (RIA) [20], MS [21] and tandem MS (MS–MS) [22] for qualitative and quantitative analyses [23]. CZE is an electrophoretic technique that may be used for substituting for, or for complementing, gel-permeation and RP-HPLC for the separation of and preparation of biological samples prior to RIA, MS and MS–MS detection. Fridland and Desiderio [24] have investigated the separation of synthetic opioid peptides by RP-HPLC based on peptide hydrophobicity. Those methods were used for analyzing peptides in human pituitaries [19,21–23].

In this present study, we investigated the separation of fourteen opioid peptides and one tachykinin peptide by CZE based on the physiochemical parameters of peptide charge and size/shape. Our investigation aims to better understand and to clarify the basic mechanisms involved in the new technique of CZE for analyzing neuropeptides in biological extracts.

2. Experimental

2.1. Reagents and materials

All synthetic opioid and tachykinin peptides were purchased from Sigma (St. Louis, MO, USA), and were used without any further purification. CZE buffers were prepared from ammonium formate (J.T. Baker, Phillipsburg, NJ, USA) or ammonium acetate (Mallinckrodt, Paris, KY, USA), and were titrated to the appropriate pH with trifluoroacetic acid (TFA; Pierce, Rockford, IL, USA) or ammonium hydroxide (Merck, Rahway, NJ, USA). Fused-silica capillary with 50 μm I.D. and 360 μm O.D. (155 μm wall thickness) was purchased from Polymicro Technologies (Phoenix, AZ, USA).

2.2. Instrumentation

CZE was performed on an ISCO Model 3140 Electropherograph (ISCO, Lincoln, NE, USA) outfitted with an IBM Personal System/2 Model 30 286 computer (IBM, Armonk, NY, USA). Peptide absorption was monitored at 200 nm using the built-in variable-wavelength UV detector. Operation of the instrument and data collection/analysis were controlled by the ISCO ICE 3.1.0 level software.

2.3. Methods

Charge calculations

The charge on each peptide was calculated using the Henderson–Hasselbach equation according to Skoog and Wichman [14]. The pK_a values for the amino and carboxyl groups of the peptide (*i.e.*, amino acids located at the N- and C-termini) and for each charged side-chain group within the peptide were obtained from a table that contained the isolated and adjusted amino acid pK_a values published by Rickard *et al.* [9]. The adjusted pK_a values were used mainly to account for the change in the electrostatic charge density that occurs on the amino acids at the N- and C-termini of a peptide. Theoretical charges were calculated across the pH range of 1 to 10 at an increment of 0.5 pH unit for each peptide using the isolated and adjusted pK_a values.

Capillary zone electrophoresis

The fused-silica capillary used was 98 cm long, with a 68 cm length from injection to the detector. The calculated surface area-to-volume ratio is 0.08. Prior to daily use, the column was preconditioned with the following sequence of solvents by applying 10 min of the electropherograph's "high vacuum" [25] from the outlet beaker for each solvent: water, 1 *M* NaOH, water, 0.1 *M* HCl, water, and finally the appropriate buffer for the experiment.

Volatile buffer systems similar to those described by others [26,27] were chosen so that samples could be further processed for MS detection. The buffers (all 20 m*M*) were ammonium formate (pH 2.5) and ammonium acetate (pH 5.5 and pH 8.5). Each individual peptide (*ca.* 1 μg; corresponding to 0.47–1.8 nmol) was dissolved in 10 μl of 1 m*M* of the appropriate buffer. The peptide mixture used in Fig. 3 also contained approximately 0.1 μg of

each peptide per μl of the 1 m*M* buffer (pH 2.5).

The applied voltage was 27 (±1%) kV, and the temperature was regulated to 30 ± 0.5°C by the electropherograph's built-in air-circulating system. Injection was done by applying vacuum from the outlet buffer reservoir. This injection volume at 30°C was calculated to be *ca.* 8 nl using the Poiseuille equation [25,28].

Ionic strength

The CZE buffers were titrated to the appropriate pH with TFA or NH_4OH. The ionic strength of the buffers at pH 2.5, 5.5 and 8.5 was calculated, based on the charge contribution of each buffer component (including the acid or base components needed to reach the desired pH value), using the pK_a values of 3.75, 4.75, 9.25 and 0.70 (value for trichloroacetic acid) for formate, acetate, ammonium and TFA, respectively [29]. The ionic strengths were 29, 20 and 20 m*M* for the three buffers at pH 2.5, 5.5 and 8.5, respectively.

Electrophoretic mobility

The experimental μ was determined as described [7]. Electroosmotic mobility at pH 2.5 was determined by using the UV absorption (10.7 min) of the internal standard $DynA_{1-13}$ ($\mu = 3.42 \cdot 10^{-4}$ cm^2/V s) [7], which is detected at 10.7 min. At pH 5.5 and 8.5, μ_{eo} values were determined by using the negative dips at 24.2 min and 7.4 min, respectively, on the electropherograms due to the migration of water in the samples [8].

3. Results and discussion

3.1. Description of peptides

Table 1 lists several features (amino acid sequence, number of basic and acidic side-chains, and M_r) of the 14 synthetic opioid peptides and 1 tachykinin peptide that were investigated in this study. The peptides range in length from 5 to 17 amino acid residues, and in M_r from 556 to 2148. Five pentapeptides (ME,

Table 1
List of the synthetic opleid and tachykinin peptides investigated in this study

Peptide (No.)	Amino acid sequence[a]	Number of basic/acidic side-chain(s)	M_r[b]
ME (14)	YGGFM	0/0	573.7
ME-K (7)	YGGFM*K*	1/0	701.8
ME[O] (15)	YGGFM[sulfoxide]	0/0	589.7
ME-NH_2 (12)	YGGFM–NH_2	0/0	572.7
ME-RGL (9)	YGGFM*R*GL	1/0	900.1
ME-RF (8)	YGGFM*R*F	1/0	877.0
LE (13)	YGGFL	0/0	555.6
LE-R (10)	YGGFL*R*	1/0	711.8
LE-K (6)	YGGFL*K*	1/0	683.8
LE-NH_2 (11)	YGGFL–NH_2	0/0	554.6
$DynA_{1-17}$ (2)	YGGFL*RRIRPKLKWDNQ*	5/1	2147.5
DynB (4)	YGGFL*RRQFKVVT*	3/0	1570.9
PreproE (5)	GG*E*VLG*KR*YGGFM	2/1	1370.6
SP (3)	*RPKP*QQFFGLM–NH_2	2/0	1347.6
$DynA_{1-13}$ (1)	YGGFL*RRIRPKLK*	5/0	1604.0

ME = Methionine enkephalin; LE = leucine enkephalin; Dyn = dynorphin; PreproE = preproenkephalin; SP = substance P.
[a] The basic residues (K,R) and acidic residues (D,E) are italicized.
[b] Molecular mass is based on the chemical mass.

ME[O], ME-NH_2, LE and LE-NH_2) have no charged side-chain group. Three hexapeptides (ME-K, LE-R and LE-K), one heptapeptide (ME-RF) and one octapeptide (ME-RGL) contain one basic side-chain group, either arginine or lysine. Five larger peptides (DynB, SP, $DynA_{1-13}$, $DynA_{1-17}$ and PreproE) contain several basic residues, but only $DynA_{1-17}$ and PreproE have a combination of basic and acidic constituents. Three peptides (ME-NH_2, LE-NH_2 and SP) have an uncharged carboxamide group. Overall, these 15 peptides range from a near zero charge to multiple positive charges at physiological pH. The combination of charges and amino acid constituents also results in the differences in the hydrophilicity and hydrophobicity of these peptides. Most importantly, the peptides investigated are representative of those neuropeptides that are under study in biological preparations [19–24].

3.2. Titration curves

To rationalize and to predict the electrophoretic separation of these 15 peptides, theoretical titration curves (of the estimate of the relative μ calculated by $q/M_r^{2/3}$) across the pH range of 1 to 10 were obtained. The isolated and adjusted amino acid pK_a values (Fig. 1A and B, respectively) were used for these plots. The three vertical lines in Fig. 1 represent the three pH values studied here. A similar approach was taken by Van de Goor *et al.* [8] in predicting and in optimizing the CZE separation of adrenocorticotropic hormone (ACTH)-related fragments, and more recently by Langenhuizen and Janssen [30] for endorphin peptide fragments.

3.3. Mass–shape term

As mentioned above, the use of the mass–shape term ($M_r^{2/3}$) assumes that an analyte's mobility in an electric field is proportional to the analyte's surface area, with an estimated spherical volume representing its size or M_r [15]. Rickard *et al.* [9] obtained a high correlation coefficient ($r = 0.989$) between electrophoretic mobilities of a human growth hormone (hGH) trypsin digest and this charge-to-mass expression. Others [3–6,10,13] have also experimentally tested and confirmed this charge-to-size parameter. The rod-shaped homopolymer model of Grossman *et al.* [7] indicates that peptide μ values also correlate well with the charge-to-mass ratio expressed by $[\ln (q + 1)]/n^{0.43}$. That homopolymer model was not used in this present study to predict electrophoretic separation, because fewer studies are available. However, it was tested with the experimental μ values. The Offord relationship was used to predict electrophoretic separation mainly because more confirmatory studies have been done, and thus more literature values are available for comparison to these present data.

Because the mass–shape parameter is assumed to be constant for each peptide across the entire pH range studied, the titration curves in Fig. 1 are solely dependent on the peptide charge across the pH range studied. As expected, the decrease in the amount of peptide charge as pH increases from acid to base is most apparent at the amino and carboxy pK_a regions, which are dominated by the C- and N-terminal amino acids for most of these peptides (Table 1). Furthermore, C- and N-terminal amino acid pK_a values are, on average, *ca.* 2.2 and 9.5, respectively, for isolated amino acids and *ca.* ten-fold less acid or base strength (3.2 and 8.1, respectively) in a peptide [9]. The shifts in the inflection points in Fig. 1A and B reflect that corresponding ten-fold decrease. Fig. 1A and B demonstrate these trends at each corresponding inflection point. The C-terminal amide peptides (ME-NH_2, LE-NH_2 and SP) do not exhibit any C-terminal amino acid ionization, and thus they maintain a constant charge until the pK_a of the N-terminal amino acid is reached.

3.4. Prediction of electrophoretic separation

The relationship between pH (and thus charge) *vs.* the $q/M_r^{2/3}$ parameter seems to be complicated, but can be rationalized readily by the ionization constants with the aid of the Henderson–Hasselbach equation. The importance of Fig. 1, however, is to predict the electrophoretic separation of these neuropep-

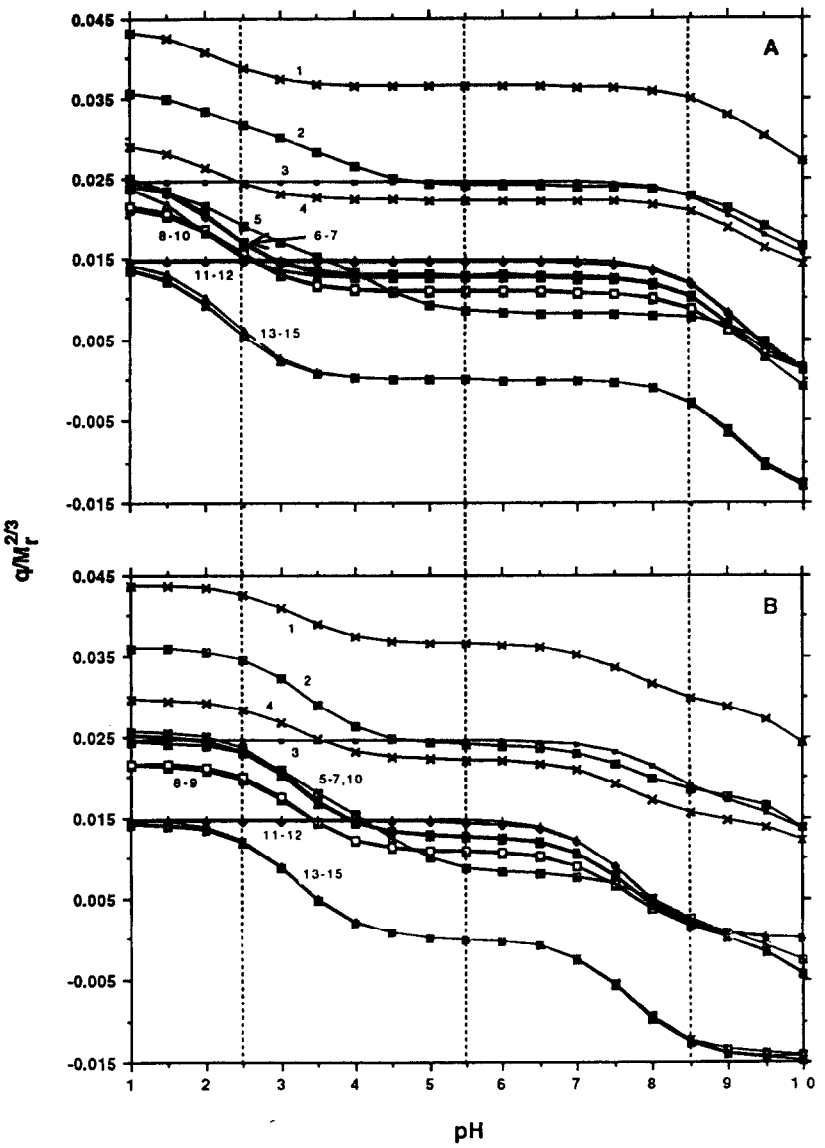

Fig. 1. The plot of $q/M_r^{2/3}$ *vs.* pH. The top figure (A) represents isolated amino acid pK_a values and the bottom (B) used adjusted pK_a values. For peptide numbering see Table 1. The vertical dashed lines indicate the three pH values (2.5, 5.5 and 8.5) studied for electrophoretic separation of these peptides.

tides. Within the three pH regions investigated (see vertical lines), the charge-to-mass differences among the peptides appear to be most diverse at pH 2.5, although differences in electrophoretic separation can be predicted from those data contained in Fig. 1A and B. For example, Fig. 1A predicts an earlier elution (*vs.* peptide 4) of peptide 3 (SP), whereas Fig. 1B predicts the opposite. Furthermore, peptides 8–9 and 11–12 are predicted to be isolated in pairs in Fig. 1B, but cluster near peptides 6–7 in Fig. 1A.

However, at pH 5.5, both plots predict a similar electrophoretic separation of all 15 peptides. [Though not very obvious from these

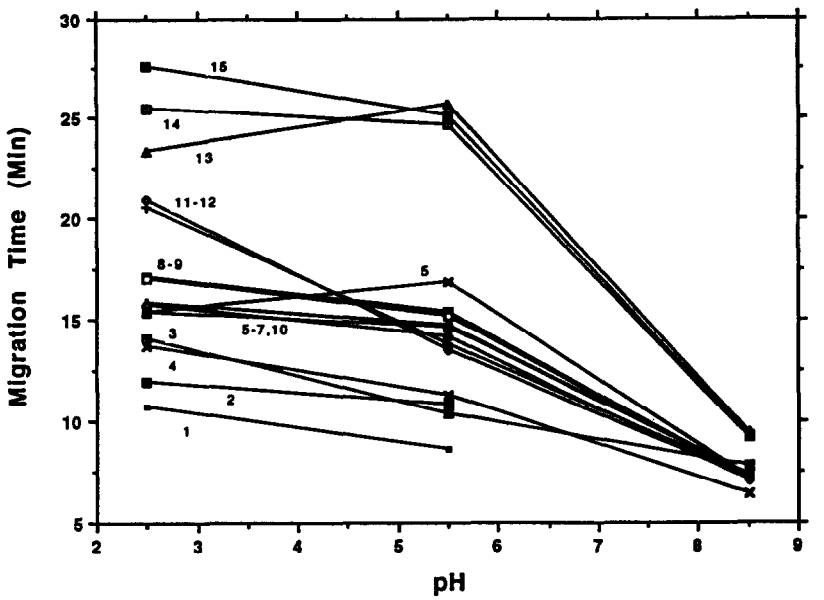

Fig. 2. Plot of electrophoretic migration time of the peptides *vs.* pH. The numbers in the figure represent the peptides listed in Table 1. $DynA_{1-13}$ (1) and $DynA_{1-17}$ (2) are missing in pH 8.5 because of analyte–wall interactions.

figures (but see later electropherogram in Fig. 3 and migration time data in Fig. 2), the electrophoretic separation of the peptides (electropherogram not shown) is less at pH 5.5.] Finally, at pH 8.5, Fig. 1A and B both predict the least electrophoretic separation (observe that the spread of the data within the 0.005–0.015 $q/M_r^{2/3}$ region is less at pH 8.5 *vs.* 5.5); Fig. 1B predicts even less separation than Fig. 1A because the amino terminus group is less ionized at that more basic pH value, according to the adjusted pK_a values. These data demonstrate that electrophoretic separation between peptides is predicted to occur when the parameter $q/M_r^{2/3}$ is $\geq ca.$ 0.004. For example, at pH 2.5, the peptides 5–7 are not predicted to separate; that prediction is correct (see Fig. 3 below).

It is also significant to correlate the sign of the charge on a peptide with pH. For example, at pH 8.5, only 3 of the 15 peptides studied could have a negative charge, and thus a negative $q/M_r^{2/3}$ parameter. Thus, ME, ME[O] and LE (peptides 13–15) are negatively charged at pH 8.5, and have a $q/M_r^{2/3}$ value of *ca.* -0.015 (see Fig. 1A and B).

3.5. Electrophoretic migration time

Fig. 2 shows the results of the electrophoretic migration times (uncorrected for electroosmosis) of the peptides individually determined at the pH values 2.5, 5.5 and 8.5. The reproducibility of the migration time of a peptide injection (fmol amounts of peptide) is typically high. For example, for the data in Fig. 2 that were obtained under these experimental conditions, the relative standard deviation (R.S.D.) is 0.13% ($n = 3$) for the multiply charged peptide SP and 0.44% ($n = 3$) for the near neutral peptide ME. This graph also demonstrates the resolution of these peptides at these pH values, and indicates that the electrophoretic migration times of any two peptides must differ by $\geq ca.$ 1 min to be resolved under these experimental conditions.

At pH 8.5, $DynA_{1-17}$ and $DynA_{1-13}$ were not detected within 30 min, presumably due to these multiply charged peptides binding to the negatively charged fused-silica wall at this pH. From Fig. 2, one can see that these 15 peptides can be best resolved at pH 2.5, because the migration times of these peptides range from *ca.* 11 to 28

min. The migration times of the peptides begin to merge (range decreases to *ca.* 8–25 min) at pH 5.5, and by pH 8.5, almost no resolution occurs (range is 7–9 min). Thus, an *ca.* 850% reduction occurred in the range of migration times of those peptides across the pH range 2.5–8.5.

Others [11,30,31] have also observed that an acidic pH is optimal for the separation of basic and neutral peptides. There are two experimental advantages of using an acidic pH to separate these peptides. First, electroosmosis is minimized, and thus the electrophoretic process is maximized; second, analyte–wall interactions are also minimized due to the protonation of silanol groups in the fused-silica wall, leading to better resolution and greater reproducibility. Thus, separation generally deteriorates more quickly than predicted (Fig. 1) as more basic pH values are used (Fig. 2).

3.6. Electropherogram data

When a mixture of all 15 peptides is injected into the capillary at pH 2.5, the electropherogram (Fig. 3) agrees very well to that separation predicted from the individual peptide migration times in Fig. 2 and with the $q/M_r^{2/3}$ parameter in Fig. 1B. All individual peptide peaks can be identified by their individual electrophoretic migration times, except for the peak that contains the mixture of ME-RF/ME-RGL (8–9) and for the peak that contains the mixture of peptides, PreproE, LE-K and ME-K (5–7).

Referring to the titration curves in Fig. 1, the observed separation of this complete mixture of the 15 peptides also agrees with the estimate of the relative μ calculated using the adjusted (Fig. 1B) *vs.* the isolated (Fig. 1A) amino acid pK_a values.

However, both titration curves in Fig. 1 fail to predict the excellent separation of peptides 13–15 at pH 2.5 shown in Figs. 2 and 3. This separation may be largely due to the fact that these peptides with a near-zero charge have undergone a significantly longer electrophoretic process, leading to greater separation. Also, specific structural features may play a role. For example, the sulfoxide group has a stronger

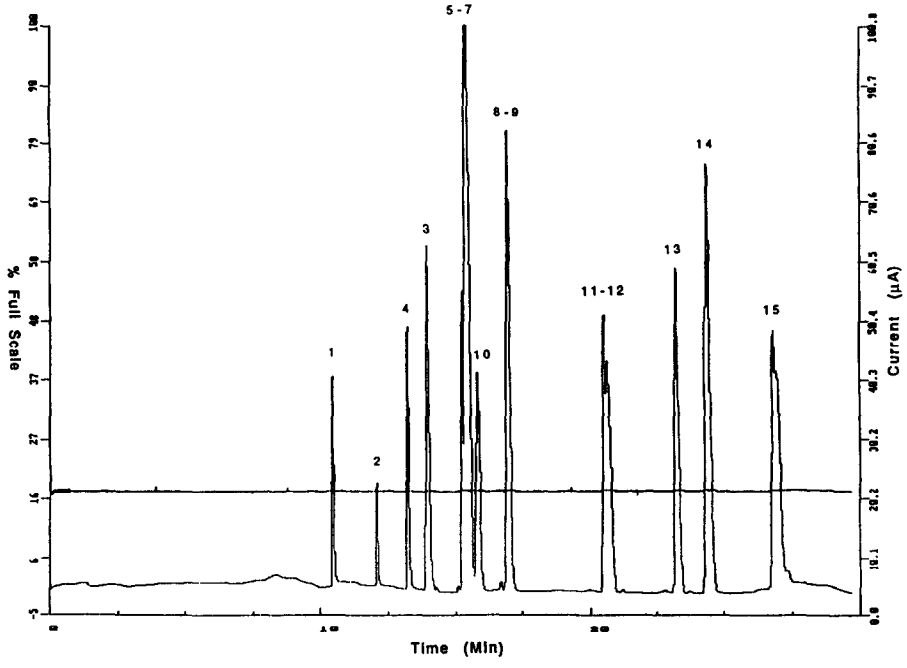

Fig. 3. Electropherogram of the peptide mixture. Numbers in the figure correspond to the peptides listed in Table 1. Separation was performed at pH 2.5. The horizontal line represents the monitored current (*ca.* 22 μA). AUFS = 0.02.

dipole than ME, ME has a polarizable sulfur atom, and LE contains neither.

3.7. Calculation of electrophoretic mobility

The migration time data collected in Fig. 2 are converted to their corresponding apparent electrophoretic mobility, based on the equation

$$\mu_{app} = v/E \quad (2)$$

where v = migration velocity (cm/s), and E = electrical field gradient (V/cm). Migration velocity is calculated by dividing the capillary length (cm) to the detector window by the migration time (s) of an analyte to reach that window. Electrical field strength is the applied voltage (V) divided by the total capillary length (cm). The calculated μ_{app} minus the μ_{eo} accounts for that portion of the peptide migration that is only due to the electrical attraction between analyte and cathode.

$$\mu = \mu_{app} - \mu_{eo} \quad (3)$$

Electroosmotic mobilities are calculated similar to peptide electrophoretic mobilities, using a small neutral molecule such as phenol or acetone [32]. Alternatively, an internal standard of known electrophoretic mobility could be included at that pH [7], or one could use the negative dip observed when the water that is contained in an injected sample migrates to the detector [8]. The measured μ_{eo} values are $4.10 \cdot 10^{-5}$ ($DynA_{1-13}$), $1.70 \cdot 10^{-4}$ (water) and $5.54 \cdot 10^{-4}$ (water) $cm^2/V\ s$ for pH 2.5, 5.5 and 8.5, respectively. As expected, the electroosmotic flow increases as pH increases to a more basic value due to the more complete ionization of the silanols on the fused-silica wall [32].

The two mass–shape parameters were tested *vs.* electrophoretic mobility. That test was done at the three pH values, and also with isolated and adjusted pK_a values. Although all of the plots that were used to test these relationships are not shown, the comparative results (linear correlation coefficients, y-intercepts and slopes) are summarized in Table 2. The results in Table 2 indicate that relatively high correlations (range: 0.928–0.997) are obtained with either mass–shape expression and with either set of amino acid pK_a values for data at any single pH value. Table 2 also provides the y-intercept and slope of each linear relationship. In general, the y-intercept is nearly zero (range: +0.0000878 to −0.000000340) in all cases in spite of the experimental difficulty in obtaining absolute electrophoretic mobilities due to the reasons discussed [9]. Only a minor variation in slopes was observed at the three pH values; however, the $q/M_r^{2/3}$ relationship gives a steeper slope (range: 0.00625–0.00882) than $[\ln(q+1)]/n^{0.43}$ (range: 0.000124–0.000643), indicating that μ is more sensitive to the $q/M_r^{2/3}$ parameter.

The degree of data scatter is least for the data set at pH 5.5 for both equations, in good agreement with the high r values obtained for that pH. That high correlation (and minimal data scatter) is readily rationalized by the titration curves in Fig. 1A and B. The greatest change in those curves obviously occurs near the inflection points (pH 2.5, 8.5), but no change at pH 5.5; thus, reproducibility is high.

Hilser *et al.* [12] performed a similar comparison at the single pH value of 2.5, using peptides obtained from the digestion with trypsin of rhIGF-I (human recombinant insulin-like growth hormone I), and reported a higher overall correlation coefficient with the homopolymer model (*e.g.* $r = 0.937$ using the adjusted amino acid pK_a values) than with the $M_r^{2/3}$ model ($r = 0.922$).

Other researchers have grouped their μ *vs.* mass–shape data that were measured within three similar pH ranges to provide a combined set of data [9]. That grouping is experimentally valid, because variables such as ionic strength, viscosity and temperature remain relatively constant over that pH range. For example, the ionic strength of the buffers used in this study at pH 2.5, 5.5 and 8.5 are 29, 20 and 20 mM, respectively. Of even greater importance is the fact that the ratio of buffer-to-analyte is *ca.* 200:1. Furthermore, μ_{eo} at pH 2.5 was determined by using $DynA_{1-13}$ (peptide 1); thus, the experimental parameters obtained at pH 2.5 (which has the highest ionic strength) are corrected for in these experiments. Thus, Table 2 also contains

Table 2
Correlation coefficients (r), y-intercepts and slopes of the electrophoretic mobility *vs.* two different equations of charge-to-mass ratio

	pH 2.5	pH 5.5	pH 8.5	Combined
$q/M_r^{2/3}$, isolated				
r^a	0.965	0.997	0.940	0.864
y-Intercept	0.0000878	−0.000000340	−0.0000699	−0.0000230
Slope	0.00685	0.00880	0.00758	0.0101
Data scatter[b]	++	+	++	+++
$q/M_r^{2/3}$, adjusted				
r^a	0.983	0.997	0.928	0.970
y-Intercept	0.0000444	−0.000000463	−0.00000916	−0.00000293
Slope	0.00751	0.00882	0.00625	0.00901
Data scatter[b]	++	+	++	++
$[\ln(q+1)]/n^{0.43}$, isolated				
r^a	0.958	0.976	0.980	0.857
y-Intercept	0.0000302	−0.0000242	−0.0000707	−0.0000473
Slope	0.000477	0.000480	0.000322	0.000539
Data scatter[b]	++	+	++	+++
$[\ln(q+1)]n^{0.43}$, adjusted				
r^a	0.984	0.976	0.985	0.857
y-Intercept	−0.0000742	−0.0000240	0.0000125	0.0000580
Slope	0.000643	0.000479	0.000124	0.000254
Data scatter[b]	++	+	++	+++

[a] Correlation coefficients of the linear least square lines.
[b] +, ++ and +++ indicate low, medium and high degree of data scatter, respectively.

the "combined" data, and Fig. 4 plots the combined data for μ *vs.* $q/M_r^{2/3}$ using adjusted pK_a values. That plot (Fig. 4) gives the best correlation ($r = 0.970$) and the least degree of data scatter *vs.* the other three combinations.

It is significant to note in Fig. 4 that three peptides, ME, ME[O] and LE, provide the three points at negative μ and negative charge ($q/M_r^{2/3}$). Those three peptides were shown above (Fig. 1) to be negatively charged at pH 8.5. These data demonstrate that μ_{eo} is greater than μ_{app} for these three peptides at pH 8.5. These three peptides are the only 3 of the 15 peptides studied (Table 1) that have a carboxylic group and no basic/acidic side-chain.

3.8. Electrophoretic mobility *vs.* pH

The correlation between μ and pH is shown by the very similar pattern obtained by compar-

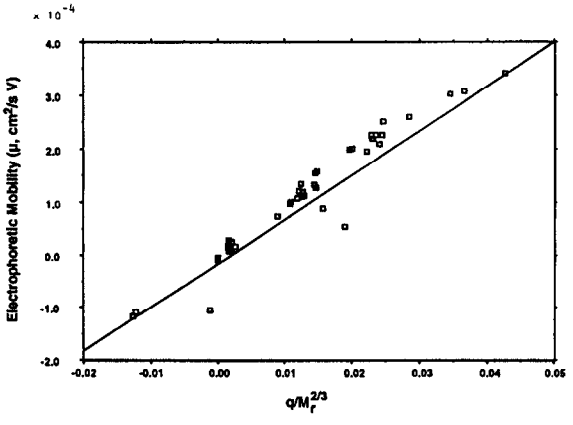

Fig. 4. Combined electrophoretic mobility measurements *vs.* $q/M_r^{2/3}$ using adjusted amino acid pK_a values over the pH range 2.5, 5.5 and 8.5. The equation of the best-fit line is $y = 0.009 - 0.000003x$ ($r = 0.970$).

ing the experimental μ (Fig. 5B) and the best-fit calculated estimate of the relative μ (Fig. 5A) plotted over the pH range studied. These μ *vs.* pH results suggest that Offord's relationship using the adjusted amino acid pK_a values of Rickard *et al.* [9] provides an additional dimension of correlation that the other three combinations fail to provide. For example, in Table 2, the combined data for rows 1 (isolated, $q/M_r^{2/3}$), and 3 and 4 (isolated and adjusted;

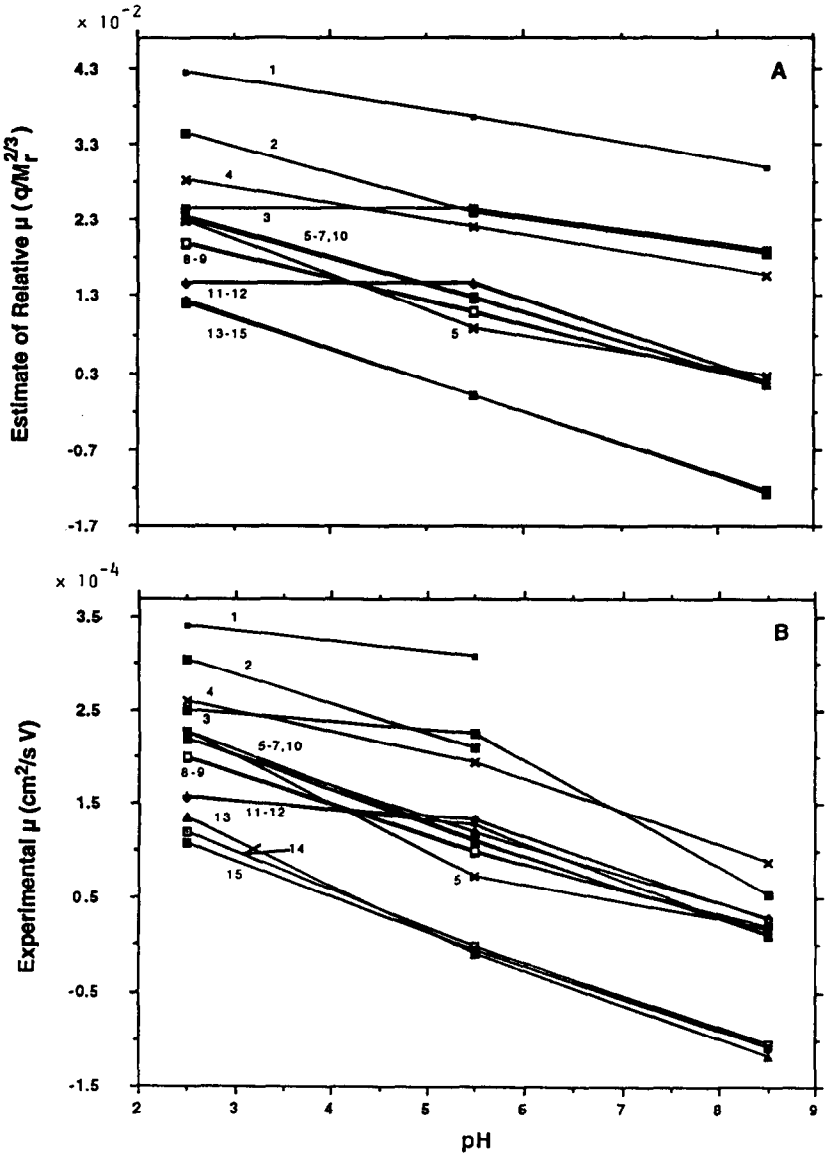

Fig. 5. Plot of experimental μ (B) and estimate of the relative μ (A) *vs.* pH. Fig. 5A correlates to Fig. 1B because only the calculations for the pH values of 2.5, 5.5 and 8.5 in Fig. 1B are shown in Fig. 5A. Fig. 5B is the experimentally determined μ at the same pH values. $DynA_{1-13}$ (1) and $DynA_{1-17}$ (2) are missing in pH 8.5 because of analyte–wall interactions.

$[\ln (q+1)]/n^{0.43}$) all have much lower r values (0.864, 0.857 and 0.857, respectively) compared to 0.970 (Fig. 4).

4. Conclusions

The separation of fourteen synthetic opioid peptides and one tachykinin peptide using CZE is demonstrated experimentally and the data are compared to several different theoretical models and factors. Data and experience derived from this study will be used to separate opioid and tachykinin peptides from human pituitary tissues and cerebrospinal fluid. A relatively wide range of pH values was investigated in this study to expand the comparison of theoretical predictions and experimental results. In general, we and others [11,28,29] conclude that neutral and basic peptides are well separated at acidic pH values such as pH 2.5, as predicted by the calculated titration curves. Furthermore, resolution is enhanced due to the low μ_{eo} and reduced analyte–wall interactions at pH 2.5. In comparing the correlation coefficient of the experimental μ *vs.* the two theoretical charge-to-mass models, one parameter, $q/M_r^{2/3}$, using adjusted amino acid pK_a values [9], provides the best overall predictable electrophoretic separation of these peptides across the wide pH range using three buffer systems. It was also demonstrated qualitatively that the titration curves obtained from the adjusted amino acid pK_a values (Fig. 1B) predict the relative electrophoretic behavior of these peptide migration times (Fig. 2) and electropherograms (Fig. 3) better than those obtained using isolated amino acid pK_a values (Fig. 1A). Although at any single pH value, the tabulated results of Table 2 suggest that $q/M_r^{2/3}$ and $[\ln (q+1)]/n^{0.43}$ both give a relatively well behaved linear relationship between the estimate of the relative μ and the experimental μ, using either set of amino acid pK_a values, the combined data indicate that $q/M_r^{2/3}$ with adjusted pK_a values provide the best correlation.

5. Acknowledgement

This work was supported by NIH GM 26666.

6. References

[1] J.W. Jorgenson and K.D. Lukacs, *Anal. Chem.*, 53 (1981) 1298.
[2] J.W. Jorgenson and K.D. Lukacs, *Science*, 222 (1983) 266.
[3] F. Nyberg, M.D. Zhu, J.L. Liao and S. Hjertén, in C. Shaefer-Nielsen (Editor), *Electrophoresis '88*, VCH, New York, 1988, p. 141.
[4] Z. Deyl, V. Rohlicek and R. Struzinsky, *J. Liq. Chromatogr.*, 12 (1989) 2515.
[5] Z. Deyl, V. Rohlicek and M. Adam, *J. Chromatogr.*, 480 (1989) 371.
[6] J. Frenz, S.-L. Wu and W.S. Hancock, *J. Chromatogr.*, 480 (1989) 379.
[7] P.D. Grossman, J.C. Colburn and H.H. Lauer, *Anal. Biochem.*, 179 (1989) 28.
[8] T.A.A.M. van de Goor, P.S.L. Janssen, J.W.V. Nispen, M.J.M.V. Zeeland and F.M. Everaerts, *J. Chromatogr.*, 545 (1991) 379.
[9] E.C. Rickard, M.M. Strohl and R.G. Nielsen, *Anal. Biochem.*, 197 (1991) 197.
[10] J.R. Florance, Z.D. Konteatis, M.J. Macielag, R.A. Lessor and A. Galdes, *J. Chromatogr.*, 559 (1991) 391.
[11] H.-J. Gaus, A.G. Beck-Sickinger and E. Bayer, *Anal. Chem.*, 65 (1993) 1399.
[12] V.J. Hilser, Jr., F.D. Worosila and S.E. Rudnick, *J. Chromatogr.*, 630 (1993) 329.
[13] H.J. Issaq, G.M. Janini, I.Z. Atamna, G.M. Muschik and J. Lukszo, *J. Liq. Chromatogr.*, 15 (1992) 1129–1142.
[14] B. Skoog and A. Wichman, *Trends Anal. Chem.*, 5 (1986) 82.
[15] R.E. Offord, *Nature*, 211 (1966) 591–593.
[16] B.L. Karger, A.S. Cohen and A. Guttman, *J. Chromatogr.*, 492 (1989) 585.
[17] Z. Deyl and R. Struzinsky, *J. Chromatogr.*, 569 (1991) 63.
[18] J.P. Landers, R.P. Oda, T.C. Spelsberg, J.A. Nolan and K.J. Ulfelder, *BioTech.*, 14 (1993) 98.
[19] J.L. Lovelace, J.J. Kusmierz and D.M. Desiderio, *J. Chromatogr.*, 562 (1991) 573.
[20] X. Zhu and D.M. Desiderio, *J. Chromatogr.*, 616 (1993) 175.
[21] J.J. Kusmierz, C. Dass, J.T. Robertson and D.M. Desiderio, *Int. J. Mass Spectrom. Ion Proc.*, 111 (1991) 247.
[22] D.M. Desiderio, J.J. Kusmierz, X. Zhu, C. Dass, D. Hilton, J.T. Robertson and H.S. Sacks, *Biol. Mass Spectrom.*, 22 (1993) 89.

[23] D.M. Desiderio, in D.M. Desiderio (Editor), *Mass Spectrometry of Peptides*, CRC Press, Boca Raton, FL, 1990.
[24] G. Fridland and D.M. Desiderio, *J. Chromatogr.*, 379 (1986) 251.
[25] H.G. Lee and D.M. Desiderio, *J. Chromatogr. B*, (1994) in press.
[26] I.M. Johansson, E.C. Huang, J.D. Henion and J. Zweigenbaum, *J. Chromatogr.*, 554 (1991) 311.
[27] M.A. Moseley, L.J. Deterding, K.B. Tomer and J.W. Jorgenson, *Anal. Chem.*, 63 (1991) 109.
[28] J. Harbaugh, M. Collette and H.E. Schwartz, *Technical Bulletin TIBC-103*, Beckman Instruments, Spinco Division, Palo Alto, CA, 1990.
[29] R.C. Weast (Editor), *CRC Handbook of Chemistry and Physics*, CRC Press, Boca Raton, FL, 70th ed., 1989, pp. D-163, D-164.
[30] M.H.J.M.L. Langenhuizen and P.S.L. Janssen, *J. Chromatogr.*, 638 (1993) 311.
[31] R.M. McCormick, *Anal. Chem.*, 60 (1988) 2322.
[32] K. Salomon, D.S. Burgi and J.C. Helmer, *J. Chromatogr.*, 559 (1991) 69.